

Supporting Information

Fused terthiophene end-capped with barbituric acid as non-fullerene n-type small molecule for green organic photo-detector

Xavier Bulliard, Gae Hwang Lee*, Tadao Yagi, Rie Sakurai, Dong-Seok Leem, Hyesung Choi, Kwang-Hee Lee, Sungyoung Yun, Jung-Hwa Kim, Daeun Yu, Youn Hee Lim, Yeong Suk Choi

Samsung Advanced Institute of Technology (SAIT), Samsung Electronics,
130 Samsung-ro, Suwon-si, Gyeong-gi-do 16678, Republic of Korea

*corresponding author: gachwang.lee@samsung.com (G. H. Lee)

Experimental procedure

The absorption spectra in solution were measured by UV-vis spectrophotometer (Shimadzu UV-240). The AFM topography height images were acquired with a Bruker Icon AFM. GIWAXS measurements were carried out at the 3C1 SAXSI beamline at Pohang Light Source II (PLS-II, Pohang). The EQE of OPD devices was measured by using a spectral incident photon-to-current efficiency (IPCE) measurement system under monochromatic light generated by an ozone-free Xe lamp with a chopper frequency of 30 Hz. Charge separation and charge collection efficiency were estimated from IQE and field-dependent PL quenching efficiency. The PL was measured by a time-correlated single photon counting (TCSPC) setup (FluoTime 300, PicoQuant GmbH) by photoexcitation with a 510-nm picosecond laser (LDH-P-C-510B, PicoQuant GmbH) operated at 40 MHz. C60 (Frontier Carbon Corp. >99.5% purity) was used as n-type material, without further purification. For the device fabrication, a 20-nm-thick hole transport layer made of molybdenum oxide (MoO_x) was deposited on an indium tin oxide (ITO)-coated glass substrate having a sheet resistance of 15 Ω per square. The active layer was prepared by vacuum thermal evaporation by co-depositing the p- and n-type materials under a pressure of 10⁻⁷ Torr. Finally the Al cathode was deposited through a shadow mask at a rate of 2 Å/s.

Synthesis of BA2T3

19.6 g (100 mmol) of dithieno[3,2-b:2',3'-d]thiophene (Sigma-Aldrich Co., Ltd.) is dissolved in 500 ml of anhydrous tetrahydrofuran (THF) under a dry nitrogen stream, and the solution is cooled down to 0°C. Then, 156 ml (250 mmol) of 1.6 M n-butyl lithium is slowly added thereto while the temperature is maintained. The reaction solution is cooled down to -78°C and agitated for one hour, and then, 22.1 g (300 mmol) of anhydrous dimethyl formamide (DMF) is dripped therein. The mixture is agitated for one hour, and the reaction solution is agitated for 2 hours until the temperature increases to room temperature. Then, the reaction solution is put in 2 L of water, and a solid remaining at the upper part after filtration during the filtration of the precipitated solid is collected and dried, obtaining 20.2 g of dithieno[3,2-b:2',3'-d]thiophene-2,6-dicarbaldehyde. (yield: 80%)

Subsequently, 1.26 g (5.0 mmol) of the dithieno[3,2-b:2',3'-d]thiophene-2,6-dicarbaldehyde and 2.34 g (15 mmol) of dimethyl barbituric acid (Sigma-Aldrich Co., Ltd.) are suspended in 60 ml of THF, piperidine (Sigma-Aldrich Co., Ltd.) in a catalytic amount is added thereto and the mixture is reacted at 50°C for 5 hours. A solid remaining at the upper part during filtration of the precipitated dark red solid is obtained and suspended in 100 ml of dimethyl acetamide (DMAc), the suspended solution is agitated at 90°C for 1 hour and the unsolved part is refiltered obtaining a solid remaining at the upper part. This process is repeated once more, obtaining 2.34 g of a compound represented by the following chemical formula BA2T3 (yield: 88.8%)

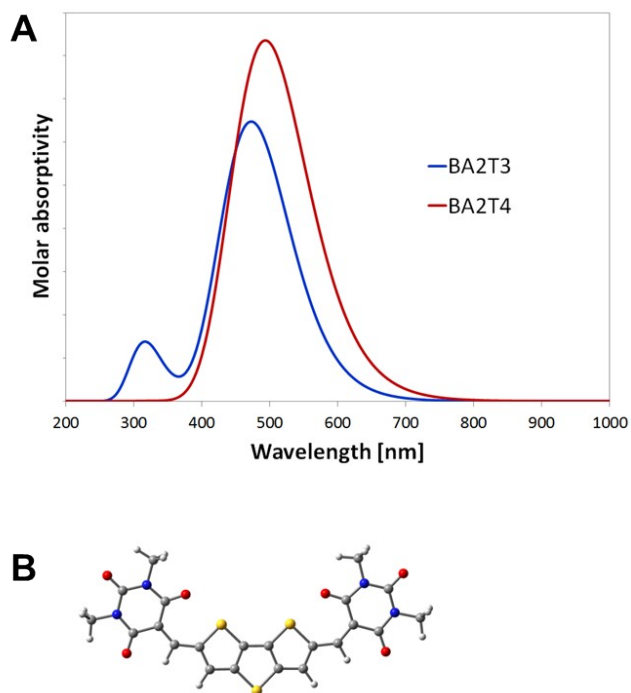


Fig. S1 (A) Absorption spectra of BA2T3 (fused terthiophene) and BA2T4 (fused quarterthiophene) calculated by TD-DFT with the B3LYP method and the 6-311G(d,p) basis set. As compared with simulation data, the maximum absorption peak position in toluene is in average red-shifted by 50 nm. (B) Minimum energy configuration calculated by DFT with the B3LYP method and the 6-311G(d,p) basis set.

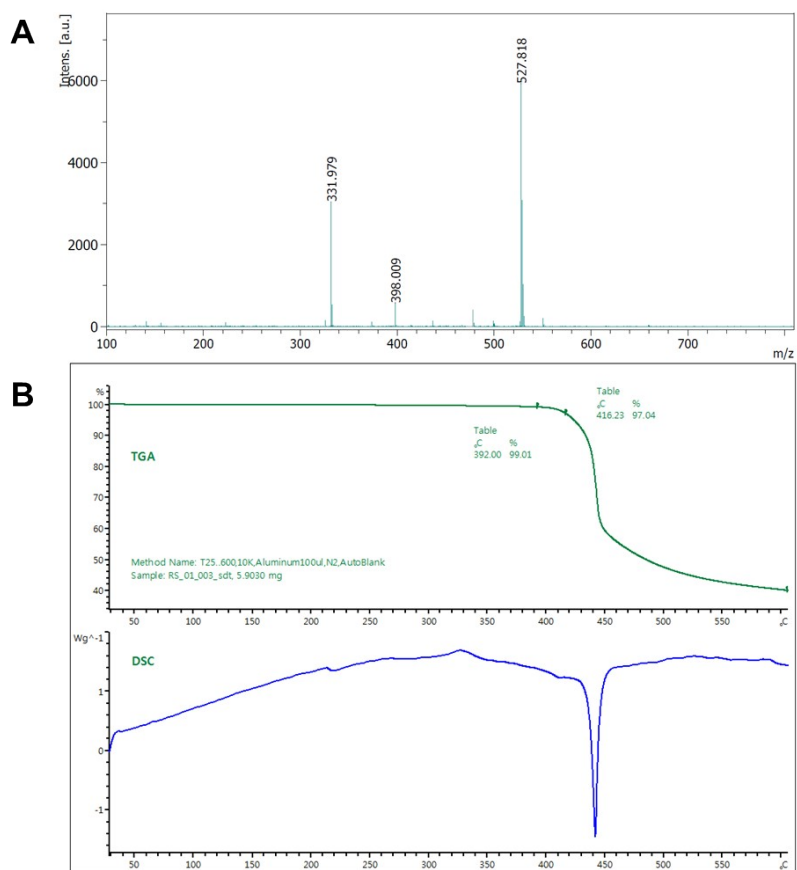


Fig. S2. (A) Maldi-ToF and (B) thermal properties of BA2T3

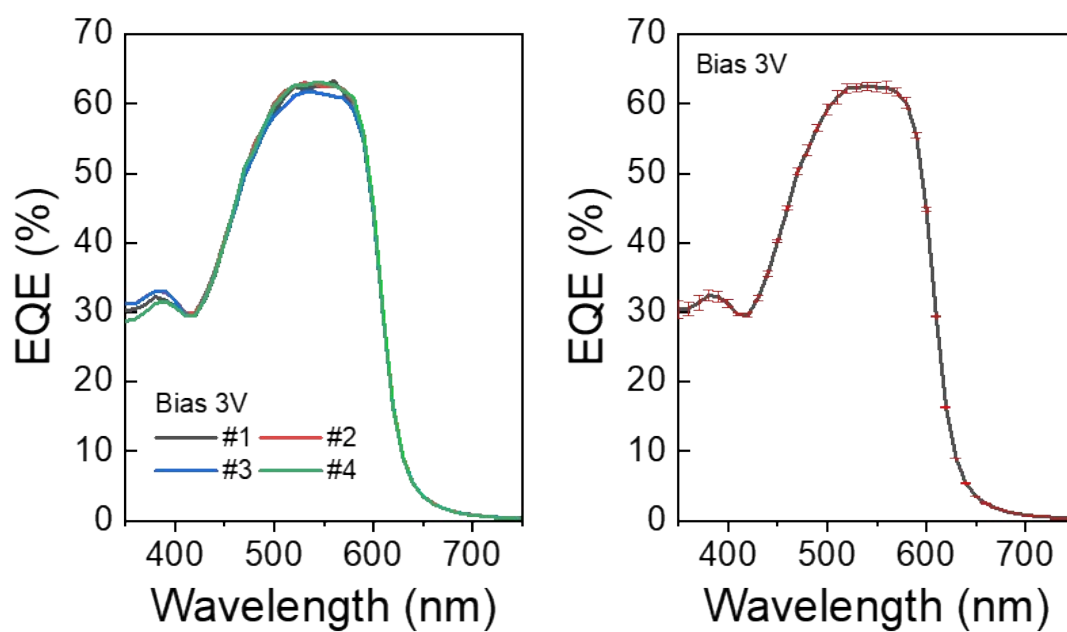


Fig. S3. Repeatable performance of OPD devices with SubPc:BA2T3 (1:1 volume ratio). The standard deviation of the EQE values was less than 1%.

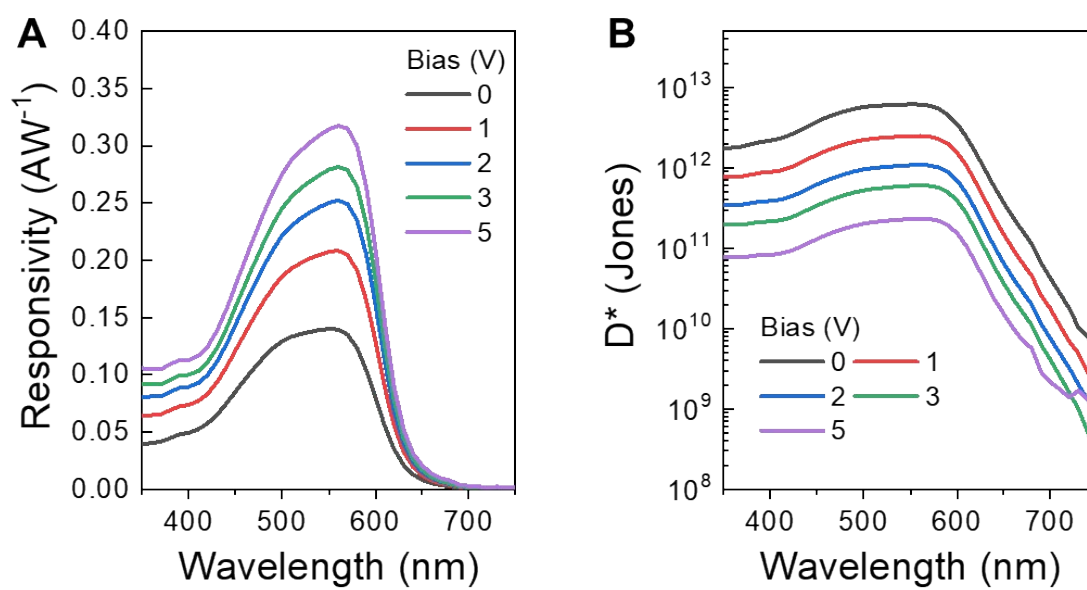


Fig. S4. Performance of OPD device with SubPc:BA2T3 (1:1 volume ratio). (A) Responsivity curves and (B) specific detectivity (D^*) with biased voltage variation from 0 to 5V.

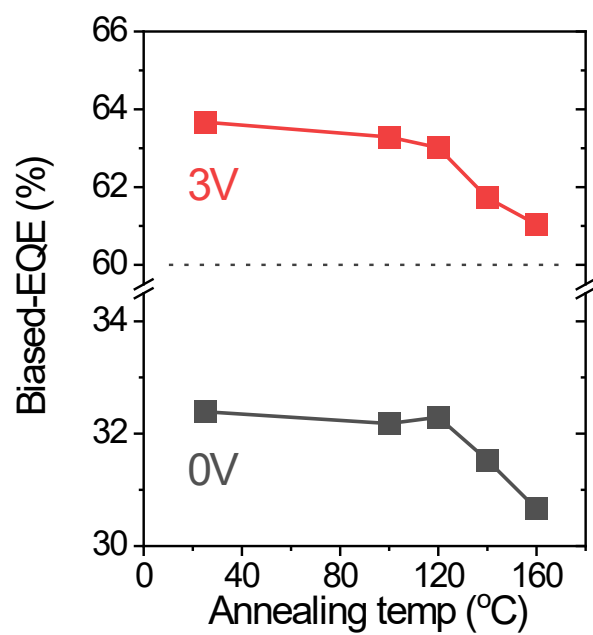


Fig. S5. Performance of OPD devices at biases of 0V and 3V with respect to the thermal annealing temperature for 1 hour. The SubPc:BA2T3 blend with a 1:1 volume ratio was used as the bulk-heterojunction active layer.

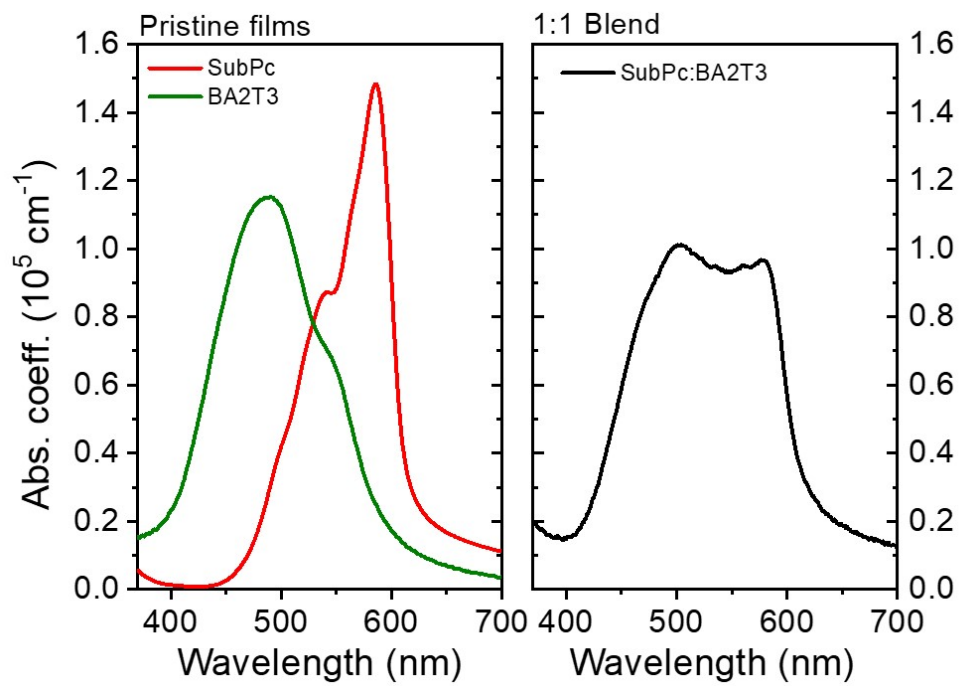


Fig. S6. Absorption spectrum of pristine films and blend film.

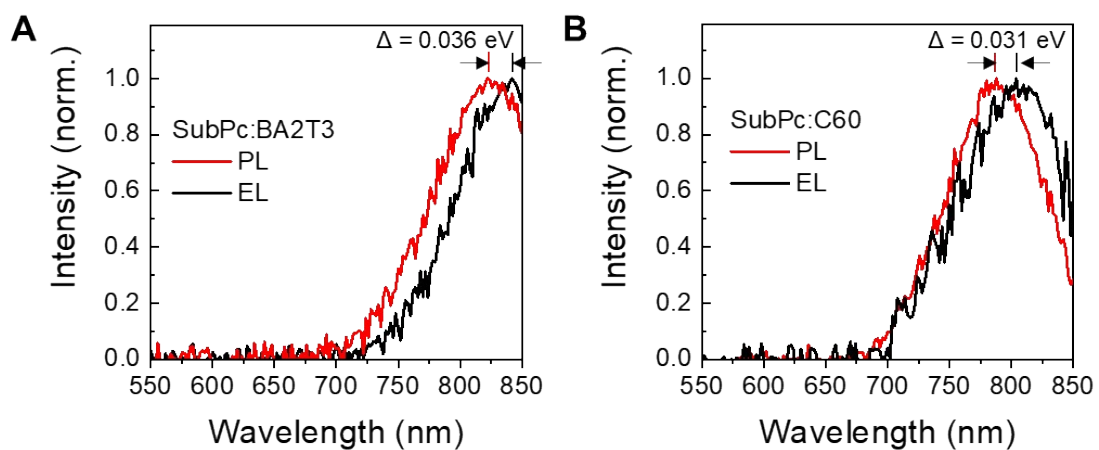


Fig. S7. Comparison of photoluminescence (PL) and electroluminescence (EL), which difference indicates carrier transport property, in (A) SubPc:BA2T3 and (B) SubPc:C60 system.

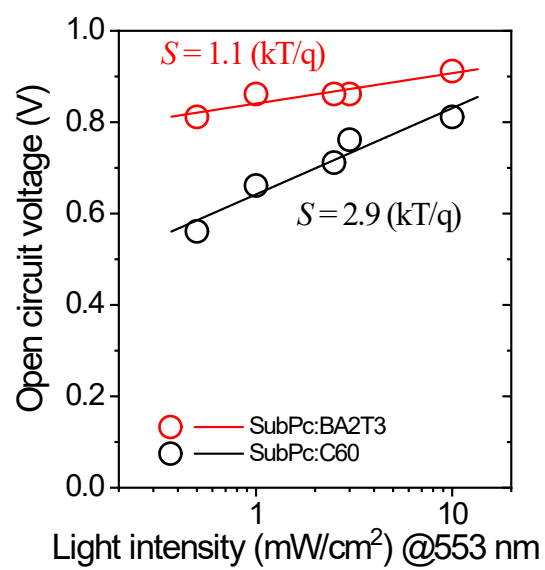


Fig. S8. Open-circuit voltage dependence on illuminance from 0.5 to 10 mW/cm² at the wavelength of 553 nm for SubPc:BA2T3 and SubPc:C60.

Table S1. Comparison of our work with previously reported non-fullerene n-type (acceptor) organic semiconductor in organic photodetectors.

a) device type: photovoltaic (PV), photodiode (PD); b) absorption of acceptor material: visible (Vis), near-infrared (NIR)

Ref.	Type ^a	Donor	Acceptor	Abs ^b	Deposition process	EQE (%)	Responsivity (A/W)	Bias (V)	Published year
[S1]	PV	PSEHTT	FTB	Vis	Solution	54	-	0	2018
	PV	PSEHTT	FTTB	Vis	Solution	84	-	0	
[S2]	PV	PTB7-Th	FDTPC-OD	NIR	Solution	63	-	0	2022
[S3]	PV	SubPc	EEB	Vis	Vacuum	38	-	0	2015
[S4]	PD	PTQ10	O-FBR	Vis	Solution	-	0.34	2	2020
[S5]	PD	PTB7-Th	IEICO-4F	NIR	Solution	-	0.12	0.5	2022
[S6]	PD	TQ-T	Y6	NIR	Solution	~16	-	2	2022
	PD	TQ-T	IEICO-4F	NIR	Solution	~14	-	2	
[S7]	PD	PM6	Y6	NIR	Solution	52	-	1	2023
	PD	PM6	3TT-FIC	NIR	Solution	54	-	1	
[S8]	PD	PM6	O4TFIC	NIR	Solution	-	0.5	0	2021
[S9]	PD	PTB7-Th	COTIC-4F	NIR	Solution	60	-	1	2022
[S10]	PD	POTB	N-PDI	Vis	Solution	-	0.017	2	2023
	PD	POTB	C-NPDI	Vis	Solution	-	0.062	2	
	PD	POTB	I-NPDI	Vis	Solution	-	0.231	2	
[S11]	PD	DMQA	SubPc	Vis	Vacuum	56.5	-	3	2015
[S12]	PD	DMQA	F5-SubPc	Vis	Vacuum	49.2	-	5	2013
	PD	SubPc	F5-SubPc	Vis	Vacuum	52.2	-	5	
This work	PD	SubPc	BA2T3	Vis (green)	Vacuum	64	0.28	3	

References

- [S1] C.-H. Tan, J. Gorman, A. Wadsworth, S. Holliday, S. Subramaniyan, S. A. Jenekhe, D. Baran, I. McCulloch and J. R. Durrant, *Chem. Commun.*, 2018, **54**, 2966.
- [S2] X. Liao, W. Xie, Z. Han, Y. Cui, X. Xia, X. Shi, Z. Yao, X. Xu, X. Lu and Y. Chen, *Adv. Funct. Mater.*, 2022, **32**, 2204255.
- [S3] P. Sullivan, G. E. Collis, L. A. Rochford, J. F. Arantes, P. Kemppinen, T. S. Jones and K. N. Winzenberg, *Chem. Commun.*, 2015, **51**, 6222-6225.
- [S4] H. Bristow, P. Jacoutot, A. D. Scaccabarozzi, M. Babics, M. Moser, A. Wadsworth, T. D. Anthopoulos, A. Bakulin, I. McCulloch and N. Gasparini, *ACS Appl. Mater. Interfaces*, 2020, **12**, 48836.
- [S5] S. Xiong, J. Li, J. Peng, X. Dong, F. Qin, W. Wang, L. Sun, Y. Xu, Q. Lin and Y. Zhou, *Adv. Opt. Mater.*, 2022, **10**, 2101837.
- [S6] P. Jacoutot, A. D. Scaccabarozzi, T. Zhang, Z. Qiao, F. Aniés, M. Neophytou, H. Bristow, R. Kumar, M. Moser, A. D. Nega, A. Schiza, A. Dimitrakopoulou-Strauss, V. G. Gregoriou, T. D. Anthopoulos, M. Heeney, I. McCulloch, A. A. Bakulin, C. L. Chochos and N. Gasparini, *Small*, 2022, **18**, 2200580.
- [S7] Y.-C. Huang, Z.-H. Huang, T.-Y. Wang, P. Chaudhary, J.-F. Hsu and K.-M. Lee, *Chem. Eng. J.*, 2023, **464**, 142633.
- [S8] M. Babics, H. Bristow, W. Zhang, A. Wadsworth, M. Neophytou, N. Gasparini and I. McCulloch, *J. Mater. Chem. C*, 2021, **9**, 2375.
- [S9] J. Simões, T. Dong and Z. Yang, *Adv. Mater. Interfaces*, 2022, **9**, 2101897.
- [S10] H. Kim, J. Kang, M. I. Kim, W. J. Jeong, S. Baek, H. Ahn, D. S. Chung and I. H. Jung, *ACS Appl. Mater. Interfaces*, 2023, **15**, 57545.
- [S11] S.-J. Lim, D.-S. Leem, K.-B. Park, K.-S. Kim, S. Sul, K. Na, G. H. Lee, C.-J. Heo, K.-H. Lee, X. Bulliard, R.-I. Satoh, T. Yagi, T. Ro, D. Im, M. Lee, T.-Y. Lee, M. G. Han, Y. W. Jin and S. Lee, *Sci. Rep.*, 2015, **5**, 7708.
- [S12] K.-H. Lee, D.-S. Leem, J. S. Castrucci, K.-B. Park, X. Bulliard, K.-S. Kim, Y. W. Jin, S. Lee, T. P. Bender and S. Y. Park, *ACS Appl. Mater. Interfaces*, 2013, **5**, 13089.